ELSEVIER

Biochimica et Biophysica Acta 1237 (1995) 6–15

BBA Biochimica et Biophysica Acta

Effect of hydration upon the fluidity of intercellular membranes of stratum corneum: an EPR study

Antonio Alonso [a,*], Nilce C. Meirelles [b], Marcel Tabak [c]

[a] *Department of Quantum Electronics, Institute of Physics, University of Campinas, Campinas 13083-970, SP, Brazil*
[b] *Department of Biochemistry, Institute of Biology, University of Campinas, Campinas 13083-970, SP, Brazil*
[c] *Institute of Chemistry, University of São Paulo, São Carlos 13560-970, SP, Brazil*

Received 1 November 1994; revised 2 February 1995; accepted 6 March 1995

Abstract

The principal mechanisms controlling the molecular permeability through the skin are associated to the intercellular membranes of stratum corneum (SC), the outermost layer of mammalian skin. It is generally accepted that an increase in fluidity of these membranes leads to a reduction of the physical barrier exerted by SC with a consequent enhancement in permeation of different compounds. It is known that water diffusion in SC increases with the increase in the water content in SC. Using the spin labeling method we evaluate the effect of hydration on the fluidity of intercellular membranes at three depths of the alkyl chain. Increase in the water content in SC leads to a drastic increase in membrane fluidity especially in the region near the membrane/water interface; the effect decreases on going deeper inside the hydrophobic core. Analysis of electron paramagnetic resonance (EPR) parameters as a function of temperature showed that the rotational motion at depth of the 16th carbon atom of the chain experienced a phase transition at 45 and 60° C. These phase transition temperatures were not altered by changes in the water content of SC. A phase transition between 28 and 48° C was observed from the segmental motion in the region near the polar headgroup (up to 12th carbon in the chain) and was strongly dependent upon the hydration of SC. Our results give a better characterization of the fluidity of SC, the main parameter involved in the mechanisms that control the permeability of different compounds through skin.

Keywords: Stratum corneum; EPR; Hydration effect; Phase transition; Membrane fluidity

1. Introduction

The intercellular lipid lamellae present in the stratum corneum (SC) constitute the main epidermal barrier to the diffusion of water and other solutes [1–5]. These lipids are arranged in multilayers between the corneocytes [6,7] and consist of ceramides (40–50%), free fatty acids (15–25%), and cholesteryl sulfate (5–10%) [8–10]. Information on molecular structure of these lipids is important for understanding diseases of SC [4] and to elaborate a rational design of effective penetration enhancers for the transdermal delivery [11]. This information has been obtained by thermal analysis [12–14], small-angle X-ray scattering [15–18], wide-angle X-ray scattering [19,20], Fourier transform infrared spectroscopy [21,22] and electron paramagnetic resonance (EPR) spectroscopy [23,24].

Several investigators [25–27] have shown that the diffusion coefficient of water in SC increases with the increase in water content. Others have suggested that water is a very effective penetration enhancer for drug permeation [28,29]. On the other hand, it is well known that both in biological and artificial membranes the permeability is increased by an increase in fluidity (for a review Ref. [30]), suggesting than a correlation between transdermal flux and lipid fluidity [31,32]. Despite this knowledge, the dynamic properties of intercellular membranes of SC are not completely characterized and the effect of hydration on the fluidity of these membranes has not been studied in detail.

The spin labeling method has been one of the most important spectroscopic methods to provide information about the dynamic structure of membranes. Considering the importance of knowledge about the structure and dy-

Abbreviations: EPR, electron paramagnetic resonance; PBS, phosphate-buffered saline; SC, stratum corneum; 5-SASL, 5-doxylstearic acid spin label; 12-SASL, 12-doxylstearic acid spin label; 16-SASL, 16-doxylstearic acid spin label.

* Corresponding author. Fax: +55 192 393127.

SSDI 0005-2736(95)00069-0

namics of intercellular membranes of SC, it is surprising that such studies are scarce, and only the spin probe perdeuterated di-*tert*-butylnitroxide (pdDTBN) has been utilized in this system [23,24]. Others probes derived from molecules that mimic the natural components of membranes can be more useful providing more complete information about the membrane.

The present investigation uses the spin labels 5-,12- and 16-doxyl stearic acid (5-, 12- and 16-SASL, respectively) in order to study the effect of hydration upon the fluidity of the intercellular membranes at three different depths of the hydrophobic chains as well as to monitor the changes in fluidity upon the temperature induced phase transitions.

2. Materials and methods

The fatty acid spin labels 5-SASL, 12-SASL and 16-SASL were purchased from Aldrich. These spin labels are stearic acid analogues and each has a nitroxide radical ring at 5th, 12th and 16th carbon position of acyl chain, respectively.

Erythrocyte ghosts were prepared from fresh human blood from normal individuals. Samples were kept on ice or under refrigeration all the way along the preparation. Red blood cells (RBC) were washed three times in phosphate-buffered saline (PBS) and hemolized in phosphate buffer 5 mM, pH 8.0. The pellet obtained after the centrifugation subsequent to hemolysis was resuspended and washed several times until white ghosts were obtained (generally 6–7 washings). The final resuspension was made in PBS and the protein concentration was measured by the method of Lowry [33]. Final protein concentration was adjusted to 10 mg/ml. Ghost membranes were labeled by adding a small aliquot of stock label solution in ethanol (5 mg/ml) in a small glass tube, evaporating the solvent under nitrogen gas flux and adding 100 μl of ghosts suspension with gentle manual agitation for 1 min. The final nitroxide concentration in the sample was $6.5 \cdot 10^{-4}$ M. In the experiments with ghosts the EPR aqueous sample cell was used.

SC was obtained from new born Wistar rats of less than 24 h of age. After killing the skin was extracted and fat is removed through the use of gaze friction in distilled water. Skin was allowed to stand for 5 min in a dissicator containing 0.5 l anhydrous ammonium hydroxide. It was then placed floating in water, with the epidermis side in contact with water, and after 2 h the SC could be removed over a filter paper and transferred to a Teflon-coated screen, where it was allowed to dry at ambient conditions. Spin labeling of SC membranes was made in an analogous way as for ghosts. A piece of 10 mg of SC (dry weight) from a single animal was ground in very small pieces and suspended in 200 μl of PBS pH 7.4 (to a final concentration of 50 mg/ml). The concentration of spin label was the same as for ghosts. After labeling the SC was introduced in a capillary for EPR measurement. The water content of the samples was estimated based on gravimetric measurements assuming that SC completely loses water on keeping for 3 days in a dissicator with 1 kg of silica. The value obtained for average and deviation was $58 \pm 7\%$ (w/w). In this work four different hydration levels were used: fully hydrated (58%), dry SC at 0–5%, obtained with dry silica, and 18 ± 2 and 33 ± 4 (w/w), obtained from carbonate solutions at 1.4 M and 3.0 M, respectively, at 31° C [26]. After EPR measurements, performed in sealed capillaries, the samples were taken from the capillary to obtain the water content.

EPR measurements were performed on a Varian E-9 spectrometer equipped with the rectangular cavity. Temperature was controlled with a nitrogen stream system from Air Products and Chemicals Inc. EPR spectra were obtained at X-band (9.150 GHz) with microwave power of 20 mW, modulation frequency 100 kHz and amplitude 2.5 G. The sweep time was 4 min and magnetic field scan 100 G.

Generally, the fluidity of a membrane can be estimated from the order parameter S which can be in the range 0–1, the lower the S values the greater the fluidity. The parameter S can be calculated from the formula of Gaffney [34]:

$$S = \frac{T'_{\parallel} - T'_{\perp} - C}{T'_{\parallel} + 2T'_{\perp} + 2C} \times 1.723 \quad (1)$$

$$C = 1.4 - 0.053(T'_{\parallel} - T'_{\perp})$$

where $T'_{\parallel}$ and $T'_{\perp}$ are the apparent parallel and perpendicular hyperfine splitting parameters of the spectrum (Fig. 1), the constant C is an empirical correction for the difference between the true and apparent polarity.

In the case of 16-SASL the calculation of S is less

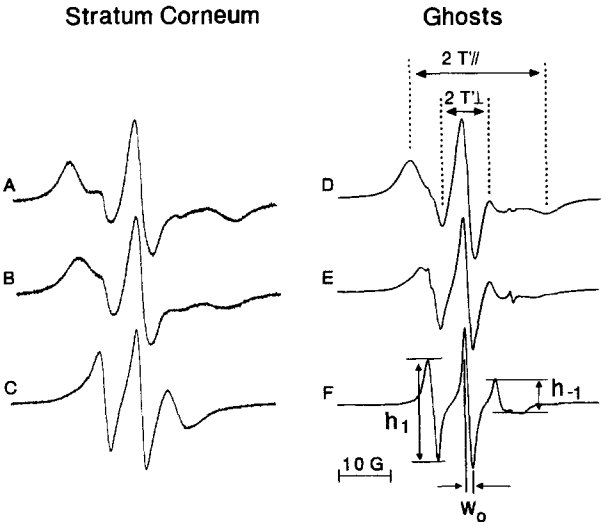

Fig. 1. EPR spectra of spin labels 5-, 12- and 16-SASL in intercellular membranes of stratum corneum (fully hydrated, A, B, C) and ghost membranes (10 mg protein/ml, D, E, F) at 37° C, both in PBS (pH 7.4). The measured parameters are indicated.

reliable since the outer features of $T'_{\|}$ are not well resolved (Fig. 1C and 1F). The $T'_{\|}$ value is calculated from the inner hyperfine splitting alone using the following relation [34]:

$$T'_{\|} = 44.5 - T'_{\perp}\,,\ C = 0.8$$

$$S(T'_{\perp}) = (43.7 - 3T'_{\perp}) \quad (2)$$

In the rapid motion regime like in the case of 16-SASL the use of the rotational correlation time τ_c can be done for the analysis of the spectra [35]:

$$\tau_c = KW_0\left((h_0/h_{-1})^{1/2} - 1\right) \quad (3)$$

$$K = 6.5 \cdot 10^{-10}\ \mathrm{s\ G^{-1}}$$

where W_0 is the peak-to-peak linewidth of the central line ($M_I = 0$), h_0 its intensity and h_{-1} is the intensity of the high field line. In order to verify the anisotropy of motion of 16-SASL in SC, rotational correlation times were calculated using two formulae based on linear and quadratic terms in the dependence of linewidth on the projection of nuclear spin [36]. The expressions used are the following:

$$\tau_{2b} = KW_0\left((h_0/h_{-1})^{1/2} - (h_0/h_{+1})^{1/2}\right) \quad (4)$$

$$\tau_{2c} = KW_0\left((h_0/h_{-1})^{1/2} + (h_0/h_{+1})^{1/2} - 2\right) \quad (5)$$

where h_{+1} is the intensity of the low field line.

The above formulae are valid for isotropic rotational diffusion. If both correlation times are equal this is an indication of isotropic motion of the spin label. The degree of anisotropy can be evaluated from the difference between the two values.

The activation energy E_a was also calculated for 16-SASL using the Arrhenius equation:

$$\log \tau_c = E_a/2.3RT \quad (6)$$

where R is the gas constant and T the absolute temperature. In practice the numerical value of E_a was determined from the slope of a plot of log τ_c versus $1/T$ (Arrhenius plot).

3. Results

The EPR spectra obtained at 37° C for 5-, 12- and 16-SASL in SC and ghost membranes are presented in Fig. 1. EPR spectra of SC are similar to typical spectra observed in plasma membranes as can be seen by comparison to EPR spectra of ghosts. The main difference is the reduced fluidity for SC membrane at this temperature. SC membranes are considered to have a low fluidity being highly ordered [2,37]. On the other hand, ghost mem-

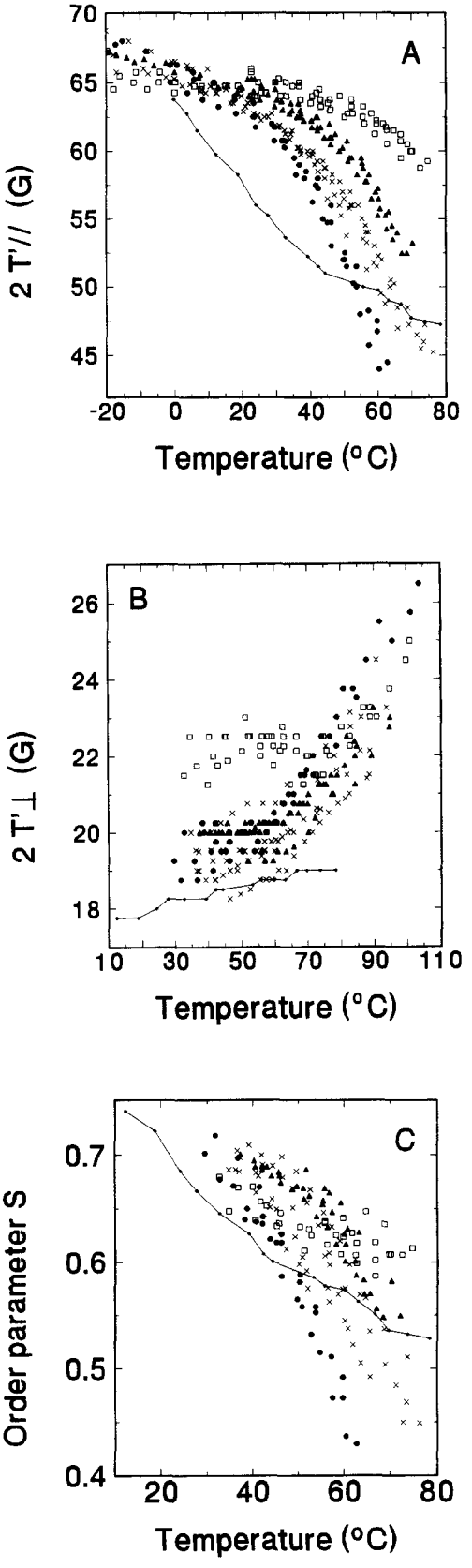

Fig. 2. EPR parameters of the spin label 5-SASL in intercellular membrane of neonatal rat stratum corneum as a function of temperature and its water content. $2T'_{\|}$, maximum hyperfine splitting and $2T'_{\perp}$, minimum hyperfine splitting as defined in Fig. 1; S, order parameter calculated from Eq. (1). Comparison is made with the probe in ghost membranes (line and smaller symbols). The water content of stratum corneum is indicated by symbols: □, 0–5% (w/w); ▲, 18% (w/w); ×, 33% (w/w); and ●, 58% (w/w).

branes, which have been the object of many studies, are also quite rigid due mostly to their high cholesterol content (20–25% of total lipids) [38], which is the same as that in SC [8–10]. Since order and fluidity may not be used always as synonyms in a simple way [39], we have compared different systems, SC and ghost membranes monitoring the changes of several parameters simultaneously.

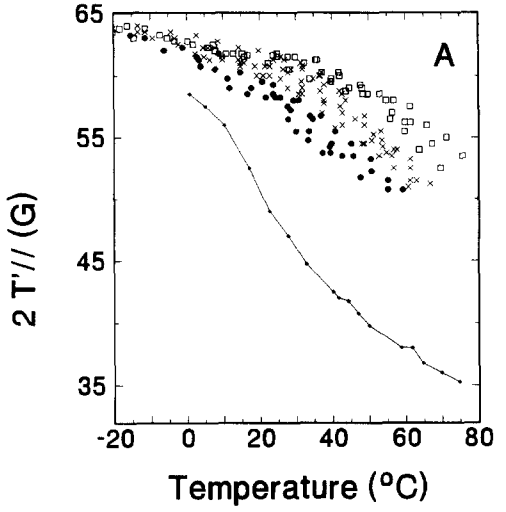

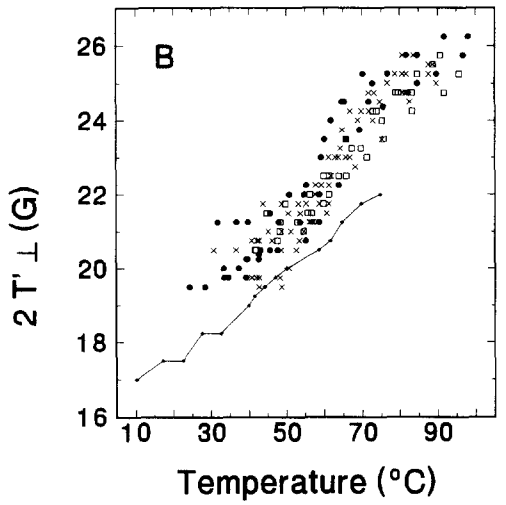

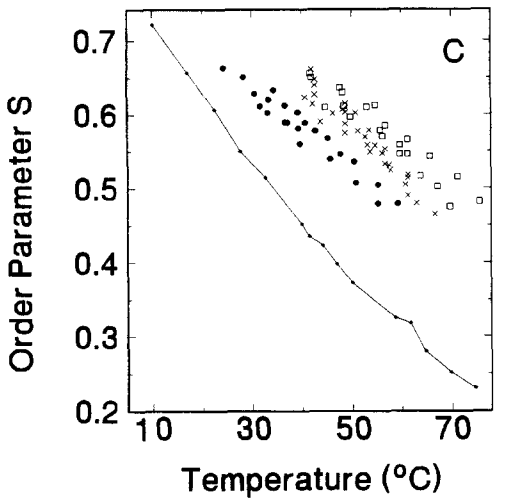

Some of these parameters like the maximum splitting or order parameter are often for brevity related to the changes in spin label mobility even though they are in principle static parameters associated to the orientational distribution of the spin labels in the membrane. Other parameters like the rotational correlation times are on the contrary directly associated with the motional reorientation of the spin labels and consequently to the probe mobility in the membrane.

In Figs. 2 and 3, the parameters $2T'_{\|}$, $2T'_{\perp}$, and S as a function of temperature are presented for 5-SASL and 12-SASL in SC and ghosts. In the SC case, four different hydration levels were measured for 5-SASL (dry, 18%, 33% and fully hydrated) while for 12-SASL three different hydrations were studied (dry, 33% and fully hydrated). Data for ghosts were included for comparison. Measurements were performed in the range from −20 to 100° C and the value of S was calculated only when $2T'_{\|}$ and $2T'_{\perp}$ are simultaneously resolved. The effect of hydration is better resolved for the parameter $2T'_{\|}$ for both nitroxides (Figs. 2A and 3A). An increase in fluidity due to hydration starts at approx. 30° C: the effect becomes more intense as the temperature increases further. This is quite dramatic comparing dry and totally hydrated SC. The effect is more pronounced for 5-SASL than for 12-SASL suggesting that at the interface close to the polar groups, where water interacts with the membrane through formation of hydrogen bonds, the changes in the motion of the spin labels are greater.

Comparing the values of $2T'_{\|}$ of 5-SASL for SC fully hydrated and ghosts (Fig. 2A) it is seen that the similarity of the two systems depends on the temperature. At 0° C and 50° C the fluidity of both samples is similar. Between 0 and 50° C the ghost membrane is more fluid than the SC membrane, and above 50° C the SC membrane becomes more fluid than the ghost membrane. In the case of 12-SASL (Fig. 3A) the fluidity of SC membrane is smaller than that for the ghost membrane in the whole temperature range.

The parameter $2T'_{\|}$ allows also the analysis of the water accessibility to the nitroxide in the membrane using the method of Griffith et al. [40]. The presence of a water hydrogen bond to the N-O fragment increases the hyperfine splitting A_{zz}. EPR spectra for frozen solutions give $2A_{zz}$. In the case of 12-SASL (Fig. 3A) the value of the

Fig. 3. EPR parameters of the spin label 12-SASL in intercellular membrane of neonatal rat stratum corneum as a function of temperature and its water content. Parameters defined as in Fig. 2. Comparison is made with the probe in ghost membranes (line and smaller symbols). The water content of stratum corneum is indicated by symbols: □, 0–5% (w/w); ×, 33% (w/w); and ●, 58% (w/w).

parameter tends to 65 G indicating a value of 32.5 G for A_{zz}, which would be the expected value for the nitroxide in a hydrophobic region in the absence of hydrogen bonds to the N-O group [40]. Thus, the absence of water can be inferred in the region of the 12th carbon in the membrane of both hydrated and dry SC. For 5-SASL (Fig. 2A) the maximum value of $2T'_{\parallel}$ tends to 69 G at $-40°$ C (not shown in the figure) when SC is fully hydrated. This would correspond to a value of A_{zz} of 34.5 G, typical for a hydrogen bonded N-O fragment of the nitroxide [40]. This suggests that in the membrane the 5-SASL has its paramagnetic fragment hydrogen bonded. In the case of dry SC this parameter tends to a value of 65 G showing that the nitroxide does not detect the presence of water in this condition.

The values of the parameter $2T'_{\perp}$ increase with the temperature (Figs. 2B and 3B). This parameter is essentially insensitive to the hydration level of SC. The unique alteration relative to hydration is observed in dry SC in the temperature range from 30 to 65° C, where this parameter increases for 5-SASL showing an unexpected high value of 22 G, constant in this temperature interval. Above 65° C this parameter has a large increase showing a dramatic increase in fluidity above this temperature.

Comparing the values of $2T'_{\perp}$ for SC totally hydrated with that for ghosts it is seen that this parameter is always greater for SC and for both nitroxides suggesting a greater fluidity in SC membranes. Although these results for $2T'_{\perp}$ are contradictory to those for $2T'_{\parallel}$ they should be regarded with great care: first of all it can be seen from Fig. 1 that in the case of ghosts membranes both $2T'_{\parallel}$ and $2T'_{\perp}$ are determined with a reasonable accuracy at 37° C while this is not the case for the SC membranes where $2T'_{\perp}$ is determined with a quite small precision. For this reason our data in Figs. 2B and 3B for $2T'_{\perp}$ are quite accurate for ghosts membranes but are inaccurate in the case of SC membranes. Besides that, and as mentioned above, the parameters $2T'_{\parallel}$ and $2T'_{\perp}$ are representative of a narrower (greater $2T'_{\parallel}$ and smaller $2T'_{\perp}$) or broader (smaller $2T'_{\parallel}$ and greater $2T'_{\perp}$) distribution of nitroxide orientations in a cone around the long symmetry axis and the association of a greater value of $2T'_{\parallel}$ with reduced fluidity is more correctly understood as a more restricted motion of the label due to a smaller cone angle with the long axis direction. In this way, we assume that results in Figs. 2A and 3A describe accurately the temperature behavior of 5-SASL and 12-SASL in the SC membrane.

The order parameter S (Fig. 2C) decreases in the whole temperature range for all samples of SC at different hydration levels. For 5-SASL, differences between the dry and hydrated conditions become apparent only above 50° C.

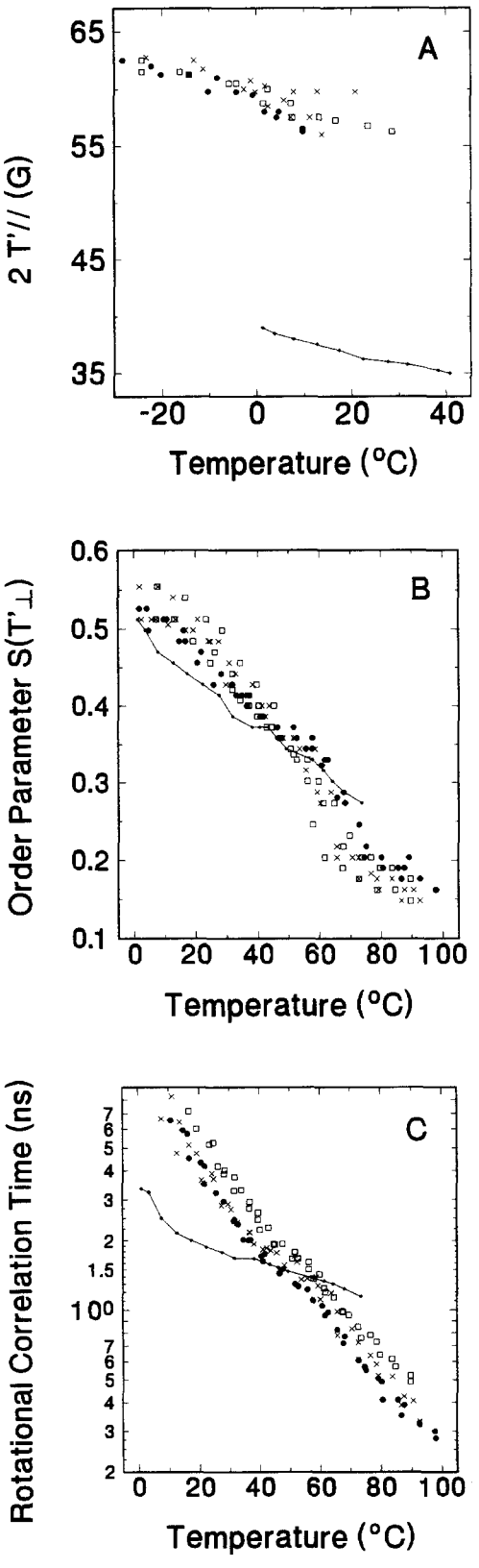

Fig. 4. EPR parameters of the spin label 16-SASL in intercellular membrane of neonatal rat stratum corneum as a function of temperature and its water content. $S(T'_{\perp})$ and τ_c were calculated from Eqs. (2) and (3), respectively. Comparison is made with the probe in ghost membranes (line and smaller symbols). The water content of stratum corneum is indicated by symbols: □, 0–5% (w/w); ×, 33% (w/w); and ●, 58% (w/w).

Water contents of 18% and 33% which are close to the ones found in vivo (10–30%) [41–45] are characterized by values of S greater than for the fully hydrated SC and above 50° C. The small differences for the S parameter at different hydration levels and low temperatures could be of course affected by the inaccuracy in the determination of $2T'_{\perp}$ which would lead to the inaccuracy in the S parameter estimation. In the case of 12-SASL (Fig. 3C) the experimental data for S show some changes as a function of hydration. The order parameter in totally hydrated SC is less than in dry SC and at hydration of 33% the obtained values are intermediate between the two extremes.

Comparison of values of S for totally hydrated SC and ghosts shows that at the polar group region (5-SASL, Fig. 2C) the order is the same in the temperature range 40–50° C; below this temperature range in SC membrane S is higher and above this range S is smaller. Above 50° C there is a significant decrease of S with temperature for SC samples at high hydration levels. On the other hand, at the C-12 position in the chain S is greater in the whole temperature range for SC, becoming closer to the values in the ghosts with increase in hydration.

In Fig. 4 the parameters $2T'_{\parallel}$, $S(T'_{\perp})$ and τ_c, rotational correlation time, for the nitroxide 16-SASL are presented as a function of temperature in SC and ghosts. In the case of SC three hydration levels are shown (dry, 33% and fully hydrated). The parameter $2T'_{\parallel}$ is not resolved in a large temperature interval within the studied range. In the temperature range 0–10° C, where this resolution is achieved, SC membranes have greater values than ghosts. At low temperature $2T'_{\parallel}$ tends to 64 G showing that the nitroxide is not sensitive to the presence of water molecules. The parameter $S(T'_{\perp})$ does not change significantly as a function of hydration of SC (Fig. 4B). In the range 45–55° C the order, S, is the same for SC and ghost membranes. Below 45° C S is slightly higher for SC membranes while above 55° C S undergoes a pronounced reduction for SC membranes. The dependence of the parameter τ_c (Fig. 4C) shows that 16-SASL in SC membranes independently of hydration is less mobile than in ghost membranes in the range 0–35° C; between 45° C and 60° C 16-SASL has the same mobility in both membranes and above 65° C the mobility of the nitroxide increases in SC membranes. This parameter indicates a slightly less mobility for dry SC as compared to fully hydrated SC.

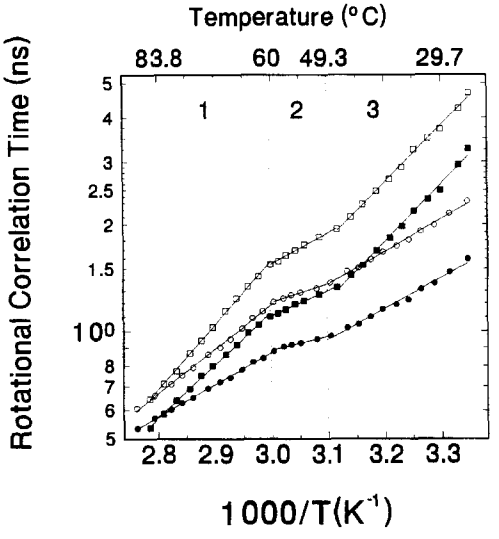

Fig. 5. Effective rotational correlation times τ_{2b} and τ_{2c} (filled and open symbols, respectively) of 16-SASL in intercellular membranes of stratum corneum plotted as a function of reciprocal absolute temperature for dry (squares) and fully hydrated stratum corneum (circles). The parameters were calculated from Eqs. (4) and (5).

Table 1
Activation energy for rotational diffusion of 16-SASL in intercellular stratum corneum membranes

Curve from	ΔE (kcal/mol)		
	region 1 [a]	region 2	region 3
Dry – τ_{2b}	$7.4\pm0.8^{A,b}$	4.3 ± 0.8^{B}	8.3 ± 0.7^{A}
Dry – τ_{2c}	9.0 ± 0.8^{A}	4.9 ± 0.8^{B}	7.9 ± 0.3^{A}
Fully hydrated – τ_{2b}	8.0 ± 0.3^{A}	4.2 ± 0.4^{B}	7.5 ± 0.7^{A}
Fully hydrated – τ_{2c}	8.6 ± 0.7^{A}	4.5 ± 0.4^{B}	7.3 ± 0.6^{A}

The means and S.D. were calculated from three independent experiments as the one presented in Fig. 5.
[a] The regions 1, 2 and 3 are indicated in Fig. 5.
[b] Statistical significance: only the means indicated with different capital letters are statistically different with $P < 0.01$ (Student's t-test).

In order to investigate the anisotropy of SC membranes, in Fig. 5 the changes in effective rotational correlation times τ_{2b} and τ_{2c} (Eqs. (4) and (5), respectively) are presented for 16-SASL in SC as a function of inverse temperature. Measurements were performed for two extreme conditions of water content (dry and fully hydrated) using SC from the same animal. It is seen that (a) the presence of water leads to a small decrease of both τ_{2b} and τ_{2c}, (b) increase of temperature makes the motion less anisotropic but even at 80° C a small difference between τ_{2b} and τ_{2c} remains, (c) some apparent changes in slopes occur showing a range of temperature, 47–60° C, where the slope is smaller, associated with a smaller activation energy. The values of activation energies calculated from

Table 2
Transition temperatures and slopes calculated from dependencies of $2T'_{\parallel}$ for 5- and 12-SASL (Figs. 2 and 3) versus $1000/T$ (K)

Water content (%)	Transition temperature (° C)		Slopes	
	5-SASL	12-SASL	5-SASL	12-SASL
0–5	$53\pm5^{A,a}$	44 ± 3^{A}	20 ± 2^{A}	24 ± 2^{A}
18±2	44 ± 2^{B}	–	41 ± 3^{B}	–
33±4	39 ± 2^{C}	33 ± 2^{B}	47 ± 6^{BC}	32 ± 3^{B}
58±7	33 ± 3^{D}	28 ± 3^{B}	51 ± 4^{C}	35 ± 2^{B}

Slopes were calculated for temperatures above the transition temperature. The means and S.D. were obtained from three independent experiments for each water content level.
[a] Statistical significance: the means in each column that do not have common capital indication letters are significantly different with $P < 0.05$ (Student's t-test).

Table 3
Rotational correlation time (τ_c) of 5-, 12- and 16-SASL for different temperatures in ghosts (10 mg protein/ml) and stratum corneum (SC) at two hydration conditions: fully hydrated – 58% (w/w) and dry – 0–5% (w/w)

Spin label	Sample	τ_c (ns)			
		30° C	45° C	60° C	75° C
5-SASL	ghosts	$12 \pm 2^{A,a}$	6.0 ± 0.8^{A}	4.9 ± 0.4^{A}	3.8 ± 0.2^{A}
	SC – hydrated	–	6.6 ± 1.2^{A}	3.7 ± 0.4^{B}	2.3 ± 0.3^{B}
	SC – dry	–	9.8 ± 0.9^{B}	5.1 ± 0.1^{A}	3.5 ± 0.2^{A}
12-SASL	ghosts	5.1 ± 0.8^{B}	3.6 ± 0.3^{C}	2.9 ± 0.2^{CD}	2.4 ± 0.2^{B}
	SC – hydrated	–	5.3 ± 0.3^{A}	2.6 ± 0.1^{D}	1.6 ± 0.2^{C}
	SC – dry	–	–	4.9 ± 1.3^{ABC}	2.4 ± 0.3^{B}
16-SASL	ghosts	1.8 ± 0.2^{C}	1.6 ± 0.1^{D}	1.4 ± 0.1^{E}	1.2 ± 0.1^{D}
	SC – hydrated	2.7 ± 0.2^{D}	1.5 ± 0.1^{D}	1.0 ± 0.1^{F}	0.5 ± 0.1^{E}
	SC – dry	3.5 ± 0.4^{E}	1.9 ± 0.1^{E}	1.4 ± 0.1^{E}	0.8 ± 0.1^{F}

The means and S.D. were obtained from three independent experiments.
[a] Statistical significance: the means in each column that do not have common capital indication letters are significantly different with $P < 0.05$ (Student's t-test).

the slopes for three independent experiments are presented in Table 1. The temperature region between 47–60° C is characterized by an activation energy of 4–5 kcal/mol, while the temperature regions below and above this interval give activation energy in the range 7–9 kcal/mol. These plots suggest that 16-SASL, that is located deep inside the membrane, experiences essentially the same energy barrier for reorientation both in low and high temperature ranges, and a smaller energy barrier for the 47–60° C interval, where probably, a phase transition may occur. This results could be explained by the increase in the intensity of the hexagonal lateral packing observed for mouse SC in the same temperature range in Ref. [20]. Since the formation of a more ordered hexagonal phase consumes energy this would explain the smaller activation energy for the motion in this temperature range.

The curves of $2T'_{\parallel}$ versus temperature for the 5- and 12-SASL (Figs. 2A and 3A) show very different slopes in low and high temperature regions (−20 to 20 and 45 to 60° C, respectively), suggesting the occurrence of phase transitions. Table 2 shows the calculated values for the transition temperatures, and the slope coefficients of the curves in the higher temperature region, as a function of the SC water content. Linear regressions of $2T'_{\parallel}$ as a function of the reciprocal absolute temperature were used in the low and high temperature limits to adjust the data. The increase in water content of SC produces significant reductions in phase transition temperatures and also increases the slopes.

At high temperature, the rate of motion is higher and the spectra allowed the measurement of the rotational correlation time for 5- and 12-SASL. These data are presented in Table 3 for SC in the two extreme conditions of hydration (dry and fully hydrated) and for ghosts. From Table 3 it is possible to point out three important characteristics. The first is that a significant difference in rotational motion between dry and fully hydrated samples of SC was observed for the three nitroxides. The second is that at 75° C the rotational motion became less restricted as the nitroxide moves away from the polar region and approaches the hydrophobic core of the membrane. For some SC samples, where the measurements were done up to 90° C, it was observed that this motion gradient remains at this temperature. The third is that around 50° C the three spin labels showed approximately the same rotational mobility for SC and ghost membranes. Below this temperature, SC membranes have lower rotational mobility and above, the mobility was higher in SC than in ghost membranes. This implies that ghost membranes remain quite rigid in the whole temperature range while in SC membranes a considerable increase in fluidity takes place at higher temperatures.

A final comment can be made about thermal transitions in ghost membranes: both nitroxides 5-SASL and 12-SASL show a unique transition in ghosts membranes as a change of slope in $2T'_{\parallel}$ and S temperature dependencies that occurs around 40° C. In the case of 16-SASL a transition for τ_c is observed of ghost membranes around 16° C.

4. Discussion

The intercellular membranes of SC can be spin labeled with nitroxides derived from stearic acid in the usual way. The EPR spectra obtained are typical for lipid bilayers. The SC membranes are considered to have low fluidity and high order [2,37]. The comparison with ghost membranes which are also quite rigid seems appropriate. Ghost membranes are certainly not a simple system, but have the advantage of being well studied and having well characterized EPR parameters for nitroxide SASL spin labels. The spectra (Fig. 1) are very similar for both SC and ghost membranes, showing only differences in the fluidity level and in the lack of resolution for $2T'_{\perp}$ for SC membranes; depending of the temperature the fluidity varies to a large extent being greater or smaller for SC membrane. On the

other hand, nitroxide reduction was not observed in our experiments (except at high temperatures, around 70° C) contrary to that observed for perdeuterated di-*tert*-butyl-nitroxide (pDTBN) [24] and with the spin labels Tempo and Tempol (unpublished data). This information can be quite important for studies of EPR imaging of skin.

The water effect is manifested more clearly for the $2T'_{\parallel}$ parameter, being larger on the polar head group and decreasing along the alkyl chain (Figs. 2A, 3A and 4A). The parameter $2T'_{\perp}$ presented high variability for the different samples and was of low sensitivity to the water effect (Figs. 2B and 3B) besides being quite inaccurate in SC. Some effect is also seen on the rotational correlation time for 16-SASL (Figs. 4C and 5). This parameter enabled the detection of the difference between the dry and fully hydrated samples. The results for the temperature dependence of rotational correlation time for 16-SASL (Figs. 4C and 5) are closely related with the data of Fourier transform infrared spectroscopy obtained by Krill et al. [22]. The curve for CH_2 symmetric stretching band position as a function of temperature shows a region of smaller slope between 42 and 60° C, while below and above this temperature interval the slope is approximately the same [22]. A similar behavior is observed for the rotational correlation time of 16-SASL (Fig. 5, Table 1), except that the temperature range of smaller slope is changed to between 47 and 60° C. We believe that some membrane reorganization may occur in this temperature range and that part of the energy transmitted to the system by raising the temperature is used for the rearrangement of lipid packing so that the response in terms of motional changes is smaller (smaller activation energies). Activation energies for reorientation of 16-SASL are independent of the hydration of SC membranes. So, it seems that water molecules do not reach the interior of SC membranes, remaining at bilayers interface.

Our results showed several apparent phase transitions for SC. The transitions observed through $2T'_{\parallel}$ measurements were sensitive to the hydration degree (Figs. 2A and 3A). On increasing the water content of SC, the transition temperature decreases, the behavior observed for numerous water-lipid systems [46], and the rate of thermal induced motion changes increases (Table 1). For the 12-SASL this rate of change is smaller than for 5-SASL, indicating that the effect is stronger near the polar head group. Below the transition temperatures, the mobility of the nitroxide moiety is hindered and the water effect is very small. Above the transition temperature, the mobility of the probe increases, with increasing rates of motion being found for the more hydrated samples and for the region close to the polar head group. So, the role of water is to promote the transition and to increase the thermally induced rate of motion.

The question on the existence of thermotropic phase transitions in the ghost membranes is controversial. The presence of a high cholesterol content has been associated to the rigidity of erythrocyte membrane and inability to undergo thermal transitions. The differential thermal calorimetry [47] or X-ray analyses [48] are unable to detect such transitions. Contrary to that, spectroscopy techniques have detected several transitions [49,50]: a transition in the range 10–20° C has been associated to a lipid phase transition, while a second transition around 40° C has been associated to the denaturation of membrane proteins. Our results show that both 5-SASL and 12-SASL are sensitive to a unique transition around 40° C which is probably due to a location of these probes in the lipid/protein interface. On the other hand, 16-SASL reports a thermal transition at 16° C which is monitored by the rotational correlation time τ_c. Since 16-SASL is deeper in the membrane it is probably reporting thermal changes in the lipid phase and for this reason only this transition at low temperature is observed.

The complexity of the lipid composition in the SC is consistent with the coexistence of several subcellular structures. Rehfeld et al. [23] have detected by differential scanning calorimetry in normal human scale unresolved endothermic phase transitions at ~ 10, ~ 28, 51–60, and 75° C. White et al. [15] studied by X-ray diffraction the structure of intercellular domains of murine SC at 25, 45 and 70° C. The wide-angle patterns indicate that only a broad band is present at 70° C, consistent with all hydrocarbon chains being in the liquid state. This broad band remains at 25 and 45° C, but additional sharp lines are seen at 25° C, characteristic of an orthorhombic-like subcell, and at 45° C, which is expected for a hexagonal subcell. The authors suggest that the small-angle pattern corresponds to the hexagonal phase at 70° C, and that the extracted lipid mixture (not the intact SC) is likely to form a hexagonal II phase, an array that consists of a hydrocarbon matrix penetrated by hexagonally packed aqueous cylinders with diameters of about 20 Å. Bouwstra et al. [20] studied the thermal behavior of murine and human SC by wide-angle X-ray scattering and observed a phase change between 20 and 45° C from an orthorhombic to a hexagonal structure for both samples. The authors also observed a disordering of the lamellar structure between 60 and 75° C and a phase change from hexagonal packing to a liquid phase in the range 75–90° C.

At 75° C, the EPR spectra for all three nitroxides in SC are characterized by a unique weakly immobilized signal, almost isotropic, and it is possible to measure the isotropic hyperfine splitting, a_0, that reflects the polarity of nitroxide environment. For the three nitroxides used, the measured value of a_0 was 14.2 G, which is typically found for the nitroxide in the membrane interior. The same value for 16-SASL was obtained in ghosts. It is of interest that 5-SASL feels the presence of water at low temperatures and at 75° C the water has no access to the nitroxide at C-5 position. This could be related to the fact that at this high temperature, 5-SASL is very soluble in the lipid moiety going deeper inside the SC membrane. On the other hand, Krill at al. [22] measured by Fourier transform infrared

spectroscopy the effect of increasing temperature on the lipid carbonyl C=O stretching vibration of hairless mice SC. The data show a decrease in the intensity of the band over the temperature range from 32 to 79° C, suggesting a more effective hydrogen bond formation of carbonyl group with water at higher temperature. From these results we can conclude that the aqueous and lipidic compartments are well separated and even if water influences the C=O bond, it has no access to the C-5 position of the nitroxide which is located deeper in the membrane.

Golden at al. [13] have observed above 70° C an abrupt increase in the water permeability of porcine SC accompanied by a large decrease in activation energy. By differential scanning calorimetry and infrared studies, the authors detected a phase transition in this tissue between 60 and 80° C. It is reasonable to assume a hexagonal II structure above 60° C, in agreement with the data from X-ray scattering [14,15] obtained for lipid extracts from other tissues; this hexagonal II structure could explain the small water diffusional barrier in the SC at 70° C [13]. The water diffusion would occur through the aqueous cylinders which exist in the hexagonal structure.

From changes in effective rotational correlation times τ_{2b} and τ_{2c} for 16-SASL (Fig. 5) it is seen that even at 80° C the motion of the nitroxide fragment is not completely isotropic. Also, it can be seen from Table 3, comparing the values of τ_c for 5-, 12-, and 16-SASL at 75° C, that the gradient of rotational motion exists and the motion increases toward the terminal methyl group of alkyl chains. These results demonstrate that in spite of the fact that the wide-angle patterns present only a broad band at 75° C for murine SC suggesting a liquid phase [15] and a change from hexagonal packing to a liquid phase in the range 75–90° C for human SC [20], it is seen that for neonatal rat SC the motion of the chains is anisotropic at 75° C. In addition, some measurements at higher temperature have shown that the anisotropy is maintained until 90° C. We believe that upon increasing the temperature to 90° C the bilayer structure is still present and is responsible for this anisotropy.

El-Shime and Princen [25] and Blank et al. [26] have shown that the coefficient of water diffusion in SC increases with the water content, approaching a constant value at a water concentration near 0.3 g/cm^3. Other investigators [28,29] have suggested that the water is a very effective penetration enhancer for drug permeation. It has been shown that biological as well as artificial membranes show increasing permeability with increasing membrane fluidity (for review see [30]), and it is known that the intercellular lipid lamellae is responsible for the epidermal permeability barrier of the SC [1–5]; so, it could be expected that water interacts with the intercellular membranes of SC, increasing its fluidity.

Our results show that the membrane fluidity increases with the water content in the neonatal rat SC. The enhancement is larger in the region near the polar headgroup layer (C-5 position) where water molecules interact with the membrane via hydrogen bonding, forming a small hydration shell that could increase the free space for segmental motion of first carbons in the alkyl chain. This interaction reducing the intermolecular forces, and probably resulting in an expansion of the membrane, also causes a small increase of the rotational motion of nitroxide at C-16 position. Above 45° C, it was possible to evaluate the τ_c parameter for the three positional isomers and the results show that this effect decreases this parameter with an increase in the rotational motion of the spin label as a whole.

These studies also show that EPR of membrane spin probes not only can provide complementary information about molecular organization and thermal behavior in SC intercellular lamellae, but can be also useful to analyze the fluidity behavior in different cases of skin diseases and lesions, or drug–lipid interactions in the SC.

Acknowledgements

This work was supported by CNPq grant process 300908/92-0 (NV) and FAPESP grant process 92/2880-0. We thank Prof. Dr. Carlos Rettori and Prof. Dr. Gaston Barberis for the support given to this work.

References

[1] Elias, P.M. and Friend, D.S. (1975) J. Cell Biol. 65, 180–191.
[2] Elias, P.M. (1981) Int. J. Derm. 20, 1–19.
[3] Wertz, P.W. and Downing D.T. (1982) Science 217, 1261–1262.
[4] Elias, P.M. (1983) J. Invest. Dermatol. 80, 44s–49s.
[5] Landman, L. (1986) J. Invest. Dermatol. 87, 202–209.
[6] Swartzendruber, D.C., Wertz, P.W., Kitko, D.J., Madison, K.C. and Downing, D.T. (1989) J. Invest. Dermatol. 92, 251–257.
[7] Wertz, P.W., Swartzendruber, D.C., Kitko, D.J., Madison, K.C. and Downing, D.T. (1989) J. Invest. Dermatol. 93, 169–172.
[8] Swartzendruber, D.C., Wertz, P.W., Madison, K.C. and Downing, D.T. (1987) J. Invest. Dermatol. 88, 709–713.
[9] Gray, G.M., White, R.J. and Yardley, H.J. (1982) Br. J. Dermatol. 106, 59–63.
[10] Long, S.A. Wertz, P.W., Strauss, J.S. and Downing, D.T. (1985) Arch. Dermatol. Res. 277, 284–287.
[11] Woodford, R. and Barry, B.W. (1986) J. Toxicol. Cutaneous Ocul. Toxicol. 5, 167– 177.
[12] Van Duzee, B.F. (1975) J. Invest. Dermatol. 65, 404–408.
[13] Golden, G.M., Guzek, D.B., Kennedy, A.H., McKie, J.E. and Potts, R.O. (1987) Biochemistry 26, 2382–2388.
[14] Bouwstra, J.A., Gooris, G.S., De Vries, M.A., Van der Spek, J.A. and Bras, W. (1992) Int. J. Pharm. 84, 205–216.
[15] White, S.H., Mirejovsky, D. and King, G.I. (1988) Biochemistry 27, 3725–3732.
[16] Bouwstra, J.A., De Vries, M.A., Gooris, G.S., Bras, W., Brussee, J. and Ponec, M. (1991) J. Contr. Rel. 15, 209–220.
[17] Garson, J.-C., Doucet, J., Leveuque, J.-L. and Tsoucaris, G. (1991) J. Invest. Dermatol. 96, 43–49.
[18] Bouwstra, J.A., Gooris, G.S., Van der Spek, J.A. and Bras, W. (1991) J. Invest. Dermatol. 97, 1005–1012.

[19] Vilkes, G.L., Nguyen, A.-L. and Wildhauer, R. (1973) Biochim. Biophys. Acta 304, 267–275.
[20] Bouwstra, J.A., Gooris, G.S., Van der Spek, J.A., Lavrijsen, S. and Bras, W. (1994) Biochim. Biophys. Acta 1212, 183–192.
[21] Bommannan, D., Potts, R.O. and Guy, R.H. (1990) J. Invest. Dermatol. 95, 403– 408.
[22] Krill, S.L., Knutson, K. and Higuchi, W.I. (1992) Biochim. Biophys. Acta 1112, 281– 286.
[23] Rehfeld, S.J., Plachy, W.Z., Williams, M.L. and Elias, P.M. (1988) J. Invest. Dermatol. 91, 499– 505.
[24] Rehfeld, S.J., Plachy, W.Z., Hou, S.Y.E. and Elias, P.M. (1990) J. Invest. Dermatol. 95, 217–223.
[25] El-Shime, A.F. and Princen, H.M. (1978) Colloid Polymer Sci. 256, 209–217.
[26] Blank, H.I., Moloney, J., Emslie, A.G., Simon, I. and Apt, C. (1984) J. Invest. Dermatol. 82, 188–194.
[27] Wu, M.-S. (1983) J. Soc. Cosmet. Chem. 34, 191–196.
[28] Potts, R.O. and Francoeur, M.L. (1991) J. Invest. Dermatol. 96, 495–499.
[29] Barry, B.W. (1987) Pharmacol. Skin 1, 121–137.
[30] Fettyplace, R. and Haydon, D.A. (1980) Physiol. Rev. 60, 510–550.
[31] Knutson, K., Potts, R.O., Guzek, D.B., Golden, G.M., Lambert, W.J., McKie, J.E. and Higuchi, W.I. (1985) J. Contr. Release 2, 67–87.
[32] Golden, G.M., McKie, J.E. and Potts, R.O. (1987) J. Pharm. Sci. 76, 25–28.
[33] Lowry, O.H., Rosebrough, N.J., Farr, A.L. and Randall, R.J. (1951) J. Biol. Chem. 193, 265–275.
[34] Gaffney, B.J. (1976) in Spin Labeling (Berliner, L.J., ed.), pp. 567–571, Academic Press, New York.
[35] Simon, I. (1979) Biochim. Biophys. Acta 556, 408–442.
[36] Berliner, L.J. (1978) Methods Enzymol. 49, 466–470.
[37] Elias, P.M., Goerke, J. and Friend, D.S. (1977) J. Invest. Dermatol. 69, 535–546.
[38] Devaux, P.F. and Seigneuret, M. (1985) Biochim. Biophys. Acta 822, 63–125.
[39] Seelig, J. (1977) Q. Rev. Biophys. 10, 353–418.
[40] Griffith, O.H., Dehlimger, P.J. and Van, S.P. (1974) J. Membr. Biol. 15, 159–192.
[41] Bulgin, J.J. and Vinson, L.T. (1977) Biochim. Biophys. Acta 136, 551–560.
[42] Foreman, M.I. (1976) Biochim. Biophys. Acta 437, 599–603.
[43] Walkley, K. (1972) J. Invest. Dermatol. 59, 225–227.
[44] Inoue, T., Tsujii, K., Okamoto, K. and Toda, K. (1986) J. Invest. Dermatol. 86, 689– 693.
[45] Takenouchi, M., Suzuki, H. and Tagami, H. (1986) J. Invest. Dermatol. 87, 574– 576.
[46] Chapman, D. (1975) Q. Rev. Biophys. 8, 185–235.
[47] Ladbrooke, B.D. and Chapman, D. (1969) Chem. Phys. Lipids 3, 304–307.
[48] Gottlieb, M.H. and Eanes, E.D. (1974) Biochim. Biophys. Acta 373, 519–522.
[49] Mihailescu, D., Constantinescu, A., Dragutan, I., Cuculescu, M. and Frangopol, P.T. (1993) Arch. Int. Physiol. Biochim. Biophys. 101, 155–159.
[50] Minetti, M., Ceccarini, M. and Di Stasi, A.M.M. (1984) J. Cell. Biochem. 25, 73–86.